Journal of Structural Engineering. Submitted June 25, 2009; accepted February 16, 2011;
posted ahead of print February 18, 2011. doi:10.1061/(ASCE)ST.1943-541X.0000398

Analysis of Structural Response of WTC 7 to Fire and Sequential Failures Leading to Collapse

Therese McAllister[1], Robert MacNeill[2], Omer Erbay[3], Andrew Sarawit[4], Mehdi Zarghamee[5]F. ASCE, Steven Kirkpatrick[6], John Gross[7]F. ASCE

1 Research Structural Engineer, PhD, PE, National Institute of Standards and Technology, Gaithersburg, MD, 20899-8611, therese.mcallister@nist.gov, 301-975-6078, fax 301-869-6275

2 Principal Engineer, Applied Research Associates, Mountain View, CA 94043

3 Senior Staff, PhD, PE, Simpson Gumpertz & Heger, Inc., Waltham, MA, 02453

4 Senior Staff, PhD, PE, Simpson Gumpertz & Heger, Inc., Waltham, MA, 02453

5 Senior Principal, PhD, PE, Simpson Gumpertz & Heger, Inc., Waltham, MA, 02453

6 Principal Engineer, PhD, Applied Research Associates, Mountain View, CA 94043

7 Research Structural Engineer, PhD, PE, National Institute of Standards and Technology, Gaithersburg, MD, 20899-8611

Abstract

This paper presents the structural analysis approach used and results obtained during the investigation conducted by National Institute of Standards and Technology (NIST) to model the sequence of fire-induced damage and failures leading to the global collapse of World Trade Center 7 (WTC 7). The structural analysis required a two-phase approach to address both the gradual response of the structure to fire before collapse initiation (approximately 4 h) and the rapid response of the structure during the collapse process (approximately 15 s). This paper emphasizes the first phase, a pseudo-static (implicit) analysis that simulated the response of structural elements to fires that spread and grew over several hours, and presents key aspects of the second phase, a dynamic (explicit) analysis that used the first phase damage as initial conditions and simulated the progression of structural failures that resulted in global collapse.

Journal of Structural Engineering. Submitted June 25, 2009; accepted February 16, 2011;
posted ahead of print February 18, 2011. doi:10.1061/(ASCE)ST.1943-541X.0000398

The analyses accounted for 1) geometric nonlinearities, 2) temperature-dependent nonlinear materials behavior for both members and connections (including thermal expansion, degradation of stiffness, yield and ultimate strength, and creep), and 3) sequential failure of structural framing and connections. Analysis uncertainty was addressed by determining rational bounds on the complex set of input conditions and by running several multi-phase analyses within those bounds. The structural response from each analysis was compared to the observed collapse behavior. This approach allowed evaluation of fire-induced damage, sequential component failures, and progression of component and subsystem failures through global collapse of WTC 7.

Keywords: World Trade Center, WTC 7, fire-induced damage, structural analysis, failure, global collapse

Journal of Structural Engineering. Submitted June 25, 2009; accepted February 16, 2011;
posted ahead of print February 18, 2011. doi:10.1061/(ASCE)ST.1943-541X.0000398

Introduction

World Trade Center 7 (WTC 7) was structurally damaged by debris during the collapse of WTC 1 at 10:28:22 a.m. eastern daylight time (EDT) on September 11, 2001. The damage included severed exterior columns on the lower floors. The collapse of WTC 1 also resulted in initiation of fires on at least 10 floors of WTC 7, extensive window breakage on the south face, and loss of city water that supplied the automatic sprinkler system in the lower floors. After hours of burning, WTC 7 collapsed at 5:20:52 p.m. EDT.

The National Institute of Standards and Technology (NIST) conducted an investigation into the collapse of the WTC buildings (NIST 2008, McAllister et al. 2008). A specific objective of the WTC investigation was to determine why and how WTC 7 collapsed. A series of detailed analyses were performed, consisting of : 1) a fire dynamics simulation to model the spread and growth of the fires with time, 2) a thermal analysis to predict the temporal and spatial distribution of temperature (temperature time-histories at every node) in the structure, and 3) a two-phased structural analysis consisting of (a) a finite element analysis to simulate the response of the structure to the fire-induced temperature histories that led to collapse initiation, and (b) a dynamic finite element analysis to simulate the sequence of subsequent structural failures that led to the collapse of the building.

Key aspects of model development and analysis results of the pseudo-static and dynamic analyses are presented. Four significant areas of uncertainty, the approach for addressing uncertainty in the analyses, and a comparison of analyses results and observed events are also presented.

Modeling Approach

Journal of Structural Engineering. Submitted June 25, 2009; accepted February 16, 2011;
posted ahead of print February 18, 2011. doi:10.1061/(ASCE)ST.1943-541X.0000398

A single software application and solution method was not available to address both the gradual response of WTC 7 to fire before collapse initiation (up to 4 hrs) and the rapid response of the structure during the collapse process (approximately 15 s). Therefore, a two-phased structural analysis approach was adopted. Figure 1 shows the sequence of analyses conducted as part of the NIST investigation of the collapse of WTC7.

In the first phase, a model was developed in ANSYS (2007) to determine the pseudo-static structural response to spatially and temporally varying fire-induced gas temperatures, and to predict the resulting local structural failures. The pseudo-static model accounted for temperature-dependent material property degradation and component failure mechanisms. Failure criteria were developed to identify when a structural component was no longer contributing to the strength or stiffness of the structural system and was removed to prevent extreme impedance of analysis convergence.

In the second phase, a companion model was developed in LS-DYNA (2007 to simulate dynamic structural response to collapse initiation and the subsequent sequential failures and load redistribution that occurred up to the global collapse of WTC 7. When sufficient damage had occurred such that the structural system appeared to be approaching instability, the fire-induced damage from the 16-story pseudo-static model and material properties corresponding to the temperatures at the time of transition were input into the 47-story dynamic model as initial conditions. The 47-story dynamic model accounted for component failures, buckling instability of columns due to loss of lateral support, dynamic effects associated with structural failures, and debris impact from falling floors.

Structural System

Journal of Structural Engineering. Submitted June 25, 2009; accepted February 16, 2011;
posted ahead of print February 18, 2011. doi:10.1061/(ASCE)ST.1943-541X.0000398

The WTC 7 building was 186 m (610 ft) high and constructed over a pre-existing electrical substation owned by Consolidated Edison. Above Floor 7, the building had typical steel framing for high-rise construction. The floor systems had steel beams acting compositely with normal weight concrete slabs on a 76 mm (3 in.) metal deck, with a total floor thickness of 140 mm (5.5 in). Figure 2 shows the floor framing and column numbering system for typical tenant floors.

Simple shear connections were used at all interior floor framing connections (i.e., beams to girders and girders to columns). The shear connections were either single shear plate, double angle, or seated connections. Single shear plate and double angle connections connected interior beams to girders and girders to interior columns. Seated connections were located at floor beam or girder connections to the exterior columns, to the north side of Column 79, and to the south side of Column 81. Moment connections were used in the exterior framing and portions of the core framing at Floors 5 and 7 as part of the lateral load resisting system. As is typical, connections in WTC 7 were not designed for loads resulting from thermal expansion effects.

16-Story Pseudo-Static Model for Structural Response to Fire-Induced Temperatures

The 16-story pseudo-static finite element model (see Figure 3) had the following features:

- Floors from ground level to Floor 16, since sustained fires were observed on Floors 7 to 9 and Floors 11 to 13 (McAllister et al. 2008).
- Representations of columns, beams, girders, composite floor slab, and connections.
- Geometric and material nonlinearities, including temperature-dependent material properties, and thermal expansion.

Journal of Structural Engineering. Submitted June 25, 2009; accepted February 16, 2011;
posted ahead of print February 18, 2011. doi:10.1061/(ASCE)ST.1943-541X.0000398

- Evolving temperature states, which included heating and cooling phases, input as a temperature time history for each node, distinct from other nodes, at 30 min intervals with linear interpolation between temperature states.
- Connection models that simulated failure of connection components.
- Failure criteria for connections, shear studs within a composite floor system, buckling instability of beams and girders, and concrete floor slabs.

Material and geometric nonlinearities were assigned to the structure between Floors 8 and 14, while Floor 7 and below and Floors 15 and 16 were modeled linearly with sub-structuring (super-elements in ANSYS) to reduce the size of the model. The gravity loads above Floor 16 were applied to the Floor 16 columns. Sub-structuring and exclusion of the building above Floor 16 allowed the analysis to remain tractable while including details of the framing and floor connections at the lower floors where fires were observed.

Beams, girders, and columns were modeled with a 3-D linear finite strain beam element (BEAM188) that is well suited for large rotation and/or large strain nonlinear solutions (ANSYS 2007). Typically, the columns were meshed with 0.6 m (2 ft) long elements, and beams were meshed with 0.9 m (3 ft) long elements. The floor slab was modeled with a 4-node finite strain shell element (SHELL181) that is well suited for large rotation and/or large strain nonlinear solutions (ANSYS 2007). Typical mesh size for the floor slab was 0.9 m x 0.9 m (3 ft x 3 ft). Temperature-dependent inelastic material properties were used for beam and shell elements.

Detailed models of floor connections and shear studs were included on the east side of Floors 8 to 14. A single-floor fire simulation performed prior to the analysis of the full structure showed that connection damage west of Columns 73 though 75 did not contribute to failures on the east side of the structure, where the collapse was observed to initiate in videos (NIST

Journal of Structural Engineering. Submitted June 25, 2009; accepted February 16, 2011;
posted ahead of print February 18, 2011. doi:10.1061/(ASCE)ST.1943-541X.0000398

NCSTAR 1A 2008). Outside of this area, structural damage, such as buckling of the steel frame and crushing and cracking of the concrete slab, was modeled, but connection failures were not modeled. Additionally, connection failures were not modeled in the exterior moment frame, as failures were not observed there prior to the onset of global collapse, or at column splices, as the purpose of the ANSYS model was to simulate local failures up to the point of buckling in a column that led to general collapse.

Connection and shear stud models were based on WTC 7 erection and fabrication shop drawings (Frankel 1985a; Frankel 1985b) and structural drawings (Cantor 1985, Cantor 1988). Their capacities were based on test data and/or calculations. Connection models were constructed with a combination of rigid beams, contact elements, control elements, spring elements, and user-defined "break elements", which modeled component failure. A control element is unidirectional and can turn on/off during an analysis to connect or disconnect parts of the connection model. A break element has a multi-degree of freedom elastic spring with the capability of disconnecting once its capacity is reached. Break elements were developed initially for the collapse analysis of the WTC 1 and WTC 2 towers (Zarghamee et al. 2005) to simulate complex modes of failure in connections using relatively few degrees of freedom.

The temperature-dependent force and moment capacity of a break element was defined with a temperature-dependent reduction factor. Different tensile and compressive capacities were assigned to connections where appropriate. Connections with multiple failure modes required several break elements connected in series and/or parallel as determined by the logical sequence of partial failures prior to the total failure of the connection. The inclusion of contact elements in the connection models allowed for slip and construction clearances (gaps) to be taken into account and thus insured different responses to tensile and compressive loads.

Journal of Structural Engineering. Submitted June 25, 2009; accepted February 16, 2011;
posted ahead of print February 18, 2011. doi:10.1061/(ASCE)ST.1943-541X.0000398

The model had approximately 101 000 elements and required the double precision version of ANSYS 11.0. Inclusion of user-defined elements prohibited parallel processing, so a 64-bit workstation was used. The analysis time was approximately 6 months for a single analysis that simulated up to 4 h of heating.

Load Application Sequence in Pseudo-Static Model

The loads applied to the model include the dead load, 25 percent of the design live load on all floors, and nodal temperature histories due to fire. Gravity loads were applied to the model in stages that simulated the sequence of construction, where the floor slab participates in the floor stiffness after the concrete has hardened. Beam camber was not included.

Temperature data were obtained from Fire Dynamics Simulator (FDS) analyses of the fires and heat transfer analyses of the heated gases to the structural components (McAllister et al. 2008). Structural elements heat slowly relative to the rapidly fluctuating gas temperatures in a fire, so component temperatures were applied incrementally in 30 min time steps for the fires observed on Floors 7 to 9 and Floors 11 to 13. The temperatures were assumed to vary linearly between consecutive steps. The temperature time histories of several floor framing and slab components on the east side of Floor 13 are shown in Figure 4.

Three different thermal cases were used in the heat transfer analyses and pseudo-static analyses. Case A used temperature data obtained from the FDS simulation of the observed fires. Cases B and C increased and decreased, respectively, the Case A gas temperature by 10 percent. These cases were within the range of realistic and reasonable fires in WTC 7 on September 11, 2001, and were judged to be within the range of uncertainty for the observed fires (McAllister et al. 2008).

Journal of Structural Engineering. Submitted June 25, 2009; accepted February 16, 2011;
posted ahead of print February 18, 2011. doi:10.1061/(ASCE)ST.1943-541X.0000398

Treatment of Failed Elements in Pseudo-Static Model

Within the ANSYS model, failure criteria were developed for addressing failed components. Members that were no longer contributing structurally to the response of the building were numerically softened or removed. This approach significantly improved computational efficiency and eliminated many convergence problems. When an element failed according to the criteria presented below, slab element stiffness was reduced to preserve the slab mass and associated live loads and beam elements were removed (the element remained in the model but contributed a near-zero stiffness).

Shear Stud Failure. Shear stud failure in composite floor systems occurs when the concrete slab crushes or cracks around the shear stud or when the shear stud separates from the steel framing. The shear strength of studs depends on rib geometry, slab thickness, concrete strength, steel strength, stud location relative to the steel deck ribs, and loading direction. Using the results from two sources, Rambo-Rodenberry (2002) and AISC (2005), the average of the strong axis and weak axis strength of shear studs was estimated to be 86.7 kN (19.5 kip). The studs failed when the load capacity, which was modified for temperature, was reached; ductility was not included for studs in the model.

Lateral-Torsional Buckling of Beams and Girders. When lateral support of the top (compression) flange was lost due to failure of the shear studs, floor beams could laterally displace and buckle in the lateral-torsional mode. However, interior girders did not have shear stud connections to the concrete slab. Therefore, girders with one-sided floor framing were also subject to lateral-torsional buckling. Buckled members were removed when the web rotation was large enough that the member would become unstable under its own gravity loading. In

Journal of Structural Engineering. Submitted June 25, 2009; accepted February 16, 2011;
posted ahead of print February 18, 2011. doi:10.1061/(ASCE)ST.1943-541X.0000398

other words, it was assumed that if a beam or girder rotated so that the flange tips were directly in line with the beam axis (i.e., the beam rotation exceeded the flange width/depth), the gravity load would have a de-stabilizing effect, and the beam or girder was removed.

Loss of Vertical Support for Beams and Girders. Under elevated temperatures, a beam could lose vertical support at its ends through connection failure, including walk-off of a beam support seat. Walk-off failure is due to either 1) movement along the axis of the beam resulting from sagging of beams or girders, or 2) lateral displacement of a girder resulting from thermal expansion of beams framing into the girder. Gravity loads in a beam are transferred to the bearing seat from the bottom flange of the beam near the web. Therefore, when the web was no longer supported by the bearing seat, the beam was assumed to have lost support, as the flexural stiffness of the bottom flange was assumed to be insufficient to transfer the gravity loads. Under such a condition, the beam was removed. While axial walk-off was possible, the computed connection failure mode was in all instances by lateral walk-off.

Cracking and Crushing of the Concrete Slab. Local temperature effects and failure of supporting beams and girders caused slab elements to undergo large compressive and tensile strains. The ANSYS material model of a concrete slab, reinforced with welded-wire-mesh, was based on an isotropic plasticity formulation without strength degradation at high strains and, hence, it could not represent cracking under tensile strains or crushing under compressive strains. To address this issue, slab elements that reached the tensile or compressive failure strains were removed.

Any slab element with a principal tensile strain equal to or greater than 0.0015 at mid-depth of the section was assumed to be fully cracked in tension. Similarly, any slab element with a principal in-plane compressive strain equal to or greater than 0.004 was considered fully

Journal of Structural Engineering. Submitted June 25, 2009; accepted February 16, 2011;
posted ahead of print February 18, 2011. doi:10.1061/(ASCE)ST.1943-541X.0000398

crushed in compressions. When these strains were reached, the concrete elastic modulus was numerically reduced to a value equivalent to the in-plane stiffness of the welded wire mesh in the slab.

The selection of failure criteria was based on experimental data and engineering mechanics, as presented above.

Structural Response to Fire in Pseudo-Static Model

Analyses of the three different thermal cases studied resulted in connection, beam, and girder failures occurring essentially at the same locations with similar failure mechanisms, but shifted in time between the three thermal cases. Case B (+10% temperatures) failures occurred at the earliest time, followed by Case A (FDS simulated temperatures), and then Case C (-10% temperatures). Only Case B results are described here.

Thermal Effects on Shear Studs and Concrete Slab. Failure of shear stud connections occurred on the east side of the building. Generally, the steel framing heated more quickly than the concrete slab. When a concrete slab section heated, cooler adjacent slab sections restrained its thermal expansion. When floor beams heated, their thermal expansion was first restrained by the shear studs and, after the shear stud connections failed, by weak axis bending of the girder. Both factors led to differential thermal expansion between the concrete slab and the floor framing. At temperatures less than approximately 400 °C (when averaged over the beam length), differential thermal expansion effects generally caused failure of shear studs along a beam length, followed by either lateral-torsional buckling of beams or girders or failure of end connections. The capacity of 28 shear studs on a floor beam in the northeast corner was estimated at about 2.4 MN (546 kip), which is less than the force produced in a fully restrained floor beam with an

Journal of Structural Engineering. Submitted June 25, 2009; accepted February 16, 2011;
posted ahead of print February 18, 2011. doi:10.1061/(ASCE)ST.1943-541X.0000398

average temperature increase of 100 ^{o}C. Therefore, shear stud connection failures were expected to occur early in the heating process.

Review of published literature did not find much data that documented shear stud connection failure in composite floors subjected to fire. One possible reason for the absence of reporting such failures in the literature is that most experimental tests of composite floor sections (a beam and slab section) have the same restraint to thermal expansion. Thus, the thermal expansion of the beam and slab are essentially the same, effectively resulting in little or no differential thermal expansion.

Thermal Effects on Floor Beams and Girder. The computed temperatures in the steel floor framing of Floor 13 at 3.0 h, 3.5 h, and 4.0 h, shown in Figure 5 (a, b, c), are largely due to heating from fire on the floor below. The corresponding computed failures of floor beams and girders of Floor 13 are shown in Figure 5 (d, e, f). (For other floors, see McAllister et al. 2008). In the east floor area, as a floor beam thermally expanded, it laterally displaced the interior girder but not the exterior framing with moment connections, which was much stiffer. Shear studs connecting the slab to the floor beam primarily failed by differential thermal expansion between the steel beams and the concrete slab. Floor beam buckling was due to the combined effects of (1) loss of lateral restraint when shear studs failed, (2) increased axial loads due to restraint of thermal expansion, and (3) gravity loads from the floor slab. Girder walk-off occurred when the beams (that framed into girders from one side) thermally expanded and pushed the girder laterally, sheared the bolts at the seated connection, and then continued to push the girder until it walked off the bearing seat. Although cooling occurred for many structural members in other parts of the structure, the beams, girders, and connections that contributed to collapse initiation had not begun cooling between 3.0 h and 4.0 h of heating (see Figure 4).

Journal of Structural Engineering. Submitted June 25, 2009; accepted February 16, 2011;
posted ahead of print February 18, 2011. doi:10.1061/(ASCE)ST.1943-541X.0000398

Thermal Effects on Connections. Thermal expansion of beams and girders caused connection failures in the form of 1) bolt shear, 2) failure of welds, and 3) walk-off of the seated connections after bolts had sheared off. Failure of bolts or welds in shear connections (single plate or double angle) resulted in loss of horizontal and vertical support to beam and girders. In seated connections, bolt failure caused loss of horizontal support, but not vertical support. Loss of vertical support occurred when the beam or girder walked off the bearing seat. Other factors that contributed to this failure were an absence of shear studs on the girders, which would have provided lateral restraint, and the one-sided framing of the east girders by the floor beams, which allowed the floor beams to push laterally on the girder when thermally expanding.

Failures Leading to Collapse Initiation in Pseudo-Static Model

The pseudo-static analyses showed that the floor framing and slabs at Floors 8 to 14 were weakened by fire after 4.0 h of heating, and Columns 79, 80, and 81 had lost lateral support at several floors. The fire-induced failures of the floor framing resulted in increased unsupported column lengths for Columns 79, 80, and 81. At this point in time, Column 79 was laterally unsupported at three floors in the east-west and north-south directions, Columns 80 was laterally unsupported at one floor in the east-west and north-south directions, and Column 81 was laterally unsupported at one floor in the north-south direction. The pseudo-static analysis simulated structural response to fire, but did not include the dynamic effects of component failures. To calculate the dynamic structural response and determine whether subsequent failures resulted in total collapse, a separate dynamic analysis was performed.

47-Story Dynamic Model of WTC 7

Journal of Structural Engineering. Submitted June 25, 2009; accepted February 16, 2011;
posted ahead of print February 18, 2011. doi:10.1061/(ASCE)ST.1943-541X.0000398

The 47-story dynamic model, shown in Figure 6, represented the steel framing, slabs, connections, and composite floor construction with shell elements. The dynamic model included as its initial condition: structural damage due to debris impact from the collapse of WTC; structural damage from pseudo static analysis; and mechanical properties for steel components for the temperature at the time of initiation of collapse. The model simulated component failure for connections and buckling of floor beams and columns; load redistribution to adjacent components; sequential failure of components and subsystems over the duration of collapse process; and dynamic effects of debris impact from falling components (MacNeill et al. 2008). To adequately capture the nonlinear behavior and failure of the structural components and subsystems, while keeping the model size tractable, typical shell element dimensions were between 150 mm (6 in.) and 300 mm (12 in.).

Modeling the behavior of floor connections was a key aspect of the structural response of WTC 7 for collapse progression. Given the shell element size limitations, the connections were modeled with a simplified geometry, and connection material models were developed to provide the expected load capacity and ductility for the dominant behaviors and failure modes.

The high number of computation cycles (millions) combined with the size of the model (3.6 million elements) required the double precision version of LS-DYNA and high-speed Linux computer clusters. The analysis time was approximately 8 weeks for a single global analysis, which simulated the structural response over approximately 15 s.

Failure Models and Criteria for Component Failures in Dynamic Model

The LS-DYNA software (Livermore 2007) allowed for the definition of failure criteria. Material failure in structural components was computed within each element based on the local

Journal of Structural Engineering. Submitted June 25, 2009; accepted February 16, 2011;
posted ahead of print February 18, 2011. doi:10.1061/(ASCE)ST.1943-541X.0000398

plastic strain. When the specified failure criterion in an element was exceeded, the element was eroded (deleted) from the calculation.

One of the significant failure modeling issues for the steel components was the effect of mesh refinement on the failure criterion. With element sizes of several inches, the local detailed damage process could not be resolved. Therefore, the measured engineering elongation of test specimens was used to set the failure strain criterion (see Kirkpatrick et al. 2005 for approach).

Connection damage and failure modes were simulated with simplified models that were developed for the expected horizontal load capacity and ductility. A nonlinear spring element was added to achieve the required vertical shear capacity of each connection while contributing minimally to horizontal capacity. Seated connections were modeled with explicit representation of the bearing seat and bolts. Sliding contact was required between the beams and plates.

Load Application Procedure in Dynamic Model

The 47-story analysis continued the pseudo-static analysis of the structural response to fire from the point in time where local instability (i.e., column buckling) appeared to be imminent. The sequence of failures was determined with the temperatures and cumulative damage from the pseudo-static analysis at 3.5 h and 4.0 h.

An initialization procedure was developed where the loads and damage were added sequentially to mimic the order in which they occurred in the building. First, gravity loads were applied gradually to minimize dynamic effects. Next, debris impact damage due to the collapse of WTC 1 was applied instantaneously to simulate the dynamic event. The analysis showed that the building remained stable and that structure above the damaged zone was able to redistribute the loads. Next, temperatures were ramped up slowly with a sinusoidal curve. Finally, fire-

Journal of Structural Engineering. Submitted June 25, 2009; accepted February 16, 2011;
posted ahead of print February 18, 2011. doi:10.1061/(ASCE)ST.1943-541X.0000398

induced damage to floor framing and connections was added instantaneously. From that point, damage was allowed to propagate and accumulate, without further input, leading to the collapse initiation event and the onset of global collapse.

The dynamic model considered elevated temperatures only at the time when damage was transferred from the pseudo-static model. The computed damage from the pseudo-static model included damage to floor beams, girders, and connections. The damage state of connections was indicated by a numerical value ranging between 0.0 for no damage (i.e., full strength remaining) and 1.0 for full damage (i.e., no strength remaining).

Failures Leading to Collapse Initiation in Dynamic Model

The dynamic analysis computed a sequence of failure events that simulated the structural response to the fire-induced damage from the pseudo-static analysis. The floor framing was thermally weakened at Floors 8 to 14, with the most substantial fire-induced damage occurring on the east side of Floors 12, 13, and 14, as Floors 11, 12, and 13 had higher combustible loads than Floors 7, 8, and 9. Floor sections on Floors 13 and 14 collapsed to the floors below. The floor systems progressively failed down to Floor 5, where debris accumulated, and left Column 79 laterally unsupported in the east-west and south directions between Floors 5 and 14. As Column 79 buckled, the column failure led to a kink in the east penthouse roof framing, which was observed in videos. A cutaway view of the structural condition surrounding Column 79 as it buckled to the east is shown in Figure 7, as well as resultant lateral displacements and column axial stress histories for Columns 79 to 81. The plots show that Column 79 began to buckle 1.3 s before the east penthouse began to descend into the building. The floor failures also led to Columns 80 and 81 buckling and floor failures across the east side of WTC 7.

Journal of Structural Engineering. Submitted June 25, 2009; accepted February 16, 2011;
posted ahead of print February 18, 2011. doi:10.1061/(ASCE)ST.1943-541X.0000398

A separate global analysis of the structure with the fire-induced damage from the pseudo-static analysis at 3.5 h (instead of 4.0 h) showed that interior columns did not buckle. The damage state at 3.5 h primarily included failure to beams and connections at the south and southeast regions of the fire affected floors.

The failures progressed westward as the debris fell and impacted adjacent intact columns and floors, until all interior columns had buckled between Floors 9 and 14. The exterior columns were left laterally unsupported in the east, south, and north faces (the west face floors remained intact above Floor 9 as no fires were observed above this floor). Exterior Column 14, adjacent to the debris impact zone, buckled first. When all exterior columns had buckled within approximately 2 s between Floors 7 and 14, as shown in Figure 8, the building above the buckled-column region moved downward, resulting in the global collapse of WTC 7.

Uncertainty Considerations and Comparison to Observable Behavior for Both Models

The WTC 7 analyses simulated the events on September 11, 2001, that were documented through photos, videos, and eyewitness accounts. Observations of actual events were used to guide the fire analyses, determine the extent of debris damage, and to validate the structural analyses. The detailed models were based on data from documents, drawings, and images, and multiple analyses were conducted for a range of input values. The analyses were executed without adjustment to input values.

Four significant areas of uncertainty influenced the analyses of WTC 7: fire growth and spread; transitioning from the structural fire response to the collapse analysis; extent of debris impact damage due to the collapse of WTC 1; and the progression of analysis from collapse initiation to global collapse.

Journal of Structural Engineering. Submitted June 25, 2009; accepted February 16, 2011;
posted ahead of print February 18, 2011. doi:10.1061/(ASCE)ST.1943-541X.0000398

Three different thermal cases were used in the pseudo-static analyses. Case A gas temperature data came from the FDS simulation of the observed fires. Cases B and C increased and decreased, respectively, the Case A gas temperature by 10 percent. This range of temperature modified the local heat transfer to the structural members, the area over which the structural members were heated, and the chance of hot zone (zone near the fire and the heated upper gas layer) overlap on adjacent floors. It became apparent as the pseudo-static analyses of the three thermal cases progressed that structural failures occurred essentially at the same locations and with similar failure mechanisms, but shifted in time between the three cases.

There was some uncertainty in selecting the time and damage state for the transition to the dynamic analyses, however, it appeared likely that the critical damage state for Case B occurred between 3.5 h and 4.0 h. The damage at 3.5 h reached a state of equilibrium after some local failures without global collapse; the damage at 4.0 h led to global collapse.

The extent of exterior structural damage to WTC 7 from debris impact during the collapse of WTC 1 (estimated from photos and videos) occurred primarily between Floors 7 and 17 in the southwest quadrant of the building. Two debris impact damage cases were used in the dynamic analyses to determine their contribution to the sequence of structural failures: (1) the observed exterior structural damage and estimated interior structural damage to floors, and (2) no structural damage from debris impact. The effect of these analyses on the sequence of structural failures is shown in Table 1, which lists the major observed collapse events with corresponding times (the start of the east penthouse descent is time zero).

Interior failures could not be ascertained from photos or videos. However, a video analysis revealed an east-west vibration of the building 6 s before the east penthouse began to move downward (see Appendix C in McAllister et. al. 2008). The vibration started at nearly the

Journal of Structural Engineering. Submitted June 25, 2009; accepted February 16, 2011;
posted ahead of print February 18, 2011. doi:10.1061/(ASCE)ST.1943-541X.0000398

time of floor failures in the dynamic analysis (6.5 s before penthouse movement). The computed time for the (1) buckling of Columns 79, 80, and 81, (2) east penthouse downward movement, and (3) descent of the east penthouse below the roofline were nearly coincident, and independent of the debris impact damage.

Interior column failures occurred over a longer duration in the analysis without debris impact damage (~ 10 s) than for the analysis with debris impact damage (~ 3 s). Without debris impact damage, the lack of core framing damage on the west side resulted in sequential failure of interior columns from east to west. With debris impact damage, the core framing damage on the west side accelerated the failure of the west interior columns.

The initial downward movement of the north face was observed at 6.9 s after the initial downward motion of the east penthouse. The two dynamic analyses straddled that value (6.3 s and 9.8 s, respectively); the case with impact damage more closely matched the observed value.

The order of the descent of the other roof structures (a screenwall and the west penthouse) below the roofline in Table 1 was reversed in the two dynamic analyses. Thus, while the computed times straddled the observed time of the screenwall and west penthouse descent into the building, the mechanisms of building decay were quite different. Without debris impact damage, the exterior columns buckled near mid-height of the building, approximately between Floors 17 and 29. With debris impact damage, the exterior columns buckled between Floors 7 to 14, due to the influence of the debris impact damage.

The uncertainty in the dynamic computations increased with the progression of the collapse sequence, due to the random nature of the debris interaction, break up, disintegration, and impact. Thus, the details of the progression of structural failures and global collapse were increasingly less certain.

Journal of Structural Engineering. Submitted June 25, 2009; accepted February 16, 2011;
posted ahead of print February 18, 2011. doi:10.1061/(ASCE)ST.1943-541X.0000398

Summary

To address the gradual response of the structure to fire before collapse initiation and the rapid collapse process, a two-phased structural analysis approach was adopted for the analysis of WTC 7. A 16-story pseudo-static finite element model simulated the response and failures of the structure to fire-induced temperature time histories. A 47-story dynamic finite element model simulated the subsequent structural failures and dynamics of the collapse process.

There were two significant features in the pseudo-static analyses and the dynamic analyses: (1) detailed connection models that captured failure of connection components, including shear studs, bolts, plates, welds, and beam walk-off from bearing seats and (2) failure criteria used to remove failed components, thus allowing simulation of sequential failures.

For the three temperature cases (Cases A, B, and C), the pseudo-static analyses had similar failure mechanisms and patterns, but were shifted in time. Case B failures occurred at the earliest time, and were used in the dynamic analyses.

The pseudo-static analyses simulated a sequence of structural failures in the fire-affected floor systems that were input into the dynamic model as initial conditions. The dynamic analyses, which also simulated falling debris impact loads, computed the collapse initiation and subsequent failures. Multiple pseudo-static and dynamic analyses that addressed four significant areas of uncertainties led to the following sequence of events: (1) collapse initiation resulted from fire-induced floor failures that led to loss of lateral support for Column 79 between Floor 5 to Floor 14; (2) column and floor failures on the east side of WTC 7 led to the failure of all interior columns through loss of lateral support and the dynamics of falling debris; (3) global collapse occurred when failure of all the core columns led to the buckling of the exterior columns.

Journal of Structural Engineering. Submitted June 25, 2009; accepted February 16, 2011;
posted ahead of print February 18, 2011. doi:10.1061/(ASCE)ST.1943-541X.0000398

Four significant areas of uncertainty were addressed by conducting multiple pseudo-static and dynamic analyses: (1) as the pseudo-static analyses progressed, the failures for three different thermal response cases were similar in location and extent, but shifted in time; (2) the dynamic analysis with fire-induced damage at 3.5 h reached a state of equilibrium after some local failures, while the analysis with fire-induced damage at 4.0 h progressed to global collapse; (3) the debris impact damage due to the collapse of WTC 1 was not a principal contributor to the collapse; (4) the uncertainty in the dynamic analyses increased with the progression of the failure sequence.

References

ANSYS. (2007). ANSYS Mechanical Release 11.0, ANSYS Inc., Southpointe, 275 Technology Drive, Canonsburg, PA, 15317.

Cantor (1985). Irwin G. Cantor P.C., Structural Engineers, Structural Drawings, 7 World Trade Center.

Cantor (1988). Irwin G. Cantor P.C., Structural Engineers, Structural Drawings for Salomon Brothers 7 World Trade Center Headquarters.

Frankel (1985a), Frankel Steel Limited, Erection Drawings, 7 World Trade Center.

Frankel (1985b), Frankel Steel Limited, Fabrication Shop Drawings, 7 World Trade Center.

Journal of Structural Engineering. Submitted June 25, 2009; accepted February 16, 2011;
posted ahead of print February 18, 2011. doi:10.1061/(ASCE)ST.1943-541X.0000398

Livermore. (2007). LS-DYNA Keyword User's Manual, Livermore Software Technology Corporation, Version 971, May.

Kirkpatrick, S. W., R. T. Bocchieri, F. Sadek, R. A. MacNeill, S. Holmes, B. D. Peterson, R. W. Cilke, C. Navarro. (2005). *Federal Building and Fire Safety Investigation of the World Trade Center Disaster: Analysis of Aircraft Impacts into the World Trade Center Towers,* NIST NCSTAR 1-2B. National Institute of Standards and Technology. Gaithersburg, MD, September, http://wtc.nist.gov/NCSTAR1/NCSTAR1-2index.htm.

McAllister, T. P., R. G. Gann, J. D. Averill, J. L. Gross, W. L. Grosshandler, J. R. Lawson, K. B. McGrattan, H. E. Nelson, W. M. Pitts, K. R. Prasad, F. H. Sadek. (2008). *Federal Building and Fire Safety Investigation of the World Trade Center Disaster: Structural Fire Response and Probable Collapse Sequence of World Trade Center Building 7.* NIST NCSTAR 1-9. National Institute of Standards and Technology. Gaithersburg, MD, November, http://wtc.nist.gov/NCSTAR1/NCSTAR1-9index.htm.

MacNeill, R., S. Kirkpatrick, B. Peterson, and R. Bocchieri, (2008). *Federal Building and Fire Safety Investigation of the World Trade Center Disaster: Global Structural Analysis of the Response of World Trade Center Building 7 to Fires and Debris Impact Damage*. NIST NCSTAR 1-9A. National Institute of Standards and Technology, Gaithersburg, MD, November, http://wtc.nist.gov/NCSTAR1/NCSTAR1-9index.htm.

Journal of Structural Engineering. Submitted June 25, 2009; accepted February 16, 2011;
posted ahead of print February 18, 2011. doi:10.1061/(ASCE)ST.1943-541X.0000398

NIST NCSTAR 1A. (2008). *Federal Building and Fire Safety Investigation of the World Trade Center Disaster: Final Report on the Collapse of the World Trade Center Building 7*, NIST, Gaithersburg, MD, November, http://wtc.nist.gov/NCSTAR1/NCSTAR1Aindex.htm.

Rambo-Roddenberry, M.D., (2002). "Behavior and Strength of Welded Stud Shear Connectors". Ph.D. thesis, Virginia Polytechnic Institute and State University, Blacksburg, VA, April 8.

Zarghamee, M. S., S. Bolourchi, D. W. Eggers, F. W. Kan, Y. Kitane, A. A. Liepins, M. Mudlock, W. I. Naguib, R. P. Ojdrovic, A. T. Sarawit, P. R Barrett, J. L. Gross, and T. P. McAllister. (2005). *Federal Building and Fire Safety Investigation of the World Trade Center Disaster: Component, Connection, and Subsystem Structural Analysis*. NIST NCSTAR 1-6C. National Institute of Standards and Technology. Gaithersburg, MD, September, http://wtc.nist.gov/NCSTAR1/NCSTAR1-6index.htm.

Journal of Structural Engineering. Submitted June 25, 2009; accepted February 16, 2011;
posted ahead of print February 18, 2011. doi:10.1061/(ASCE)ST.1943-541X.0000398

List of Tables

Table 1. Comparison of major collapse events: observed times versus analysis times for collapse analyses with and without debris impact damage.

List of Figures

Figure 1. WTC 7 analysis sequence (McAllister et. al. 2008). Note : Certain commercial software or materials are identified to describe a procedure or concept adequately. Such identification is not intended to imply recommendation, endorsement, or implication by NIST that the software or materials are necessarily the best available for the purpose.

Figure 2. Floors 8 through 45 framing plan with column numbering.

Figure 3. 16-story pseudo-static model representing lower 16 floors of the WTC 7 building. The nonlinear part of the model subjected to thermal loading is shown in blue (McAllister et. al. 2008).

Figure 4. Temperature time-history of selected floor framing and slab at Floor 13..

Figure 5. Floor 13 framing temperatures at (a) 3.0 h, (b) 3.5 h, and (c) 4.0 h. (Temperature scale range: 0 ºC to 675 ºC; temperatures > 675 ºC are grey.) ANSYS floor 13 beam and girder failures (by buckling or end connection damage) at (d) 3.0 h, (e) 3.5 h, and (f) 4.0 h (McAllister et. al. 2008).

Figure 6. 47-story model of the WTC 7 building with debris impact damage, with damage at southwest corner (McAllister et. al. 2008).

Figure 7. Column 79 and 81 stress and displacements (McAllister et. al. 2008). Note: the collapse reference time of zero (0.0 s) is the point in time when the east penthouse structure on the roof of WTC 7 began to move downward.

Figure 8. Exterior column buckling after initiation of global collapse with debris impact and fire-induced damage (slabs removed from view) (McAllister et. al. 2008).

Journal of Structural Engineering. Submitted June 25, 2009; accepted February 16, 2011;
posted ahead of print February 18, 2011. doi:10.1061/(ASCE)ST.1943-541X.0000398

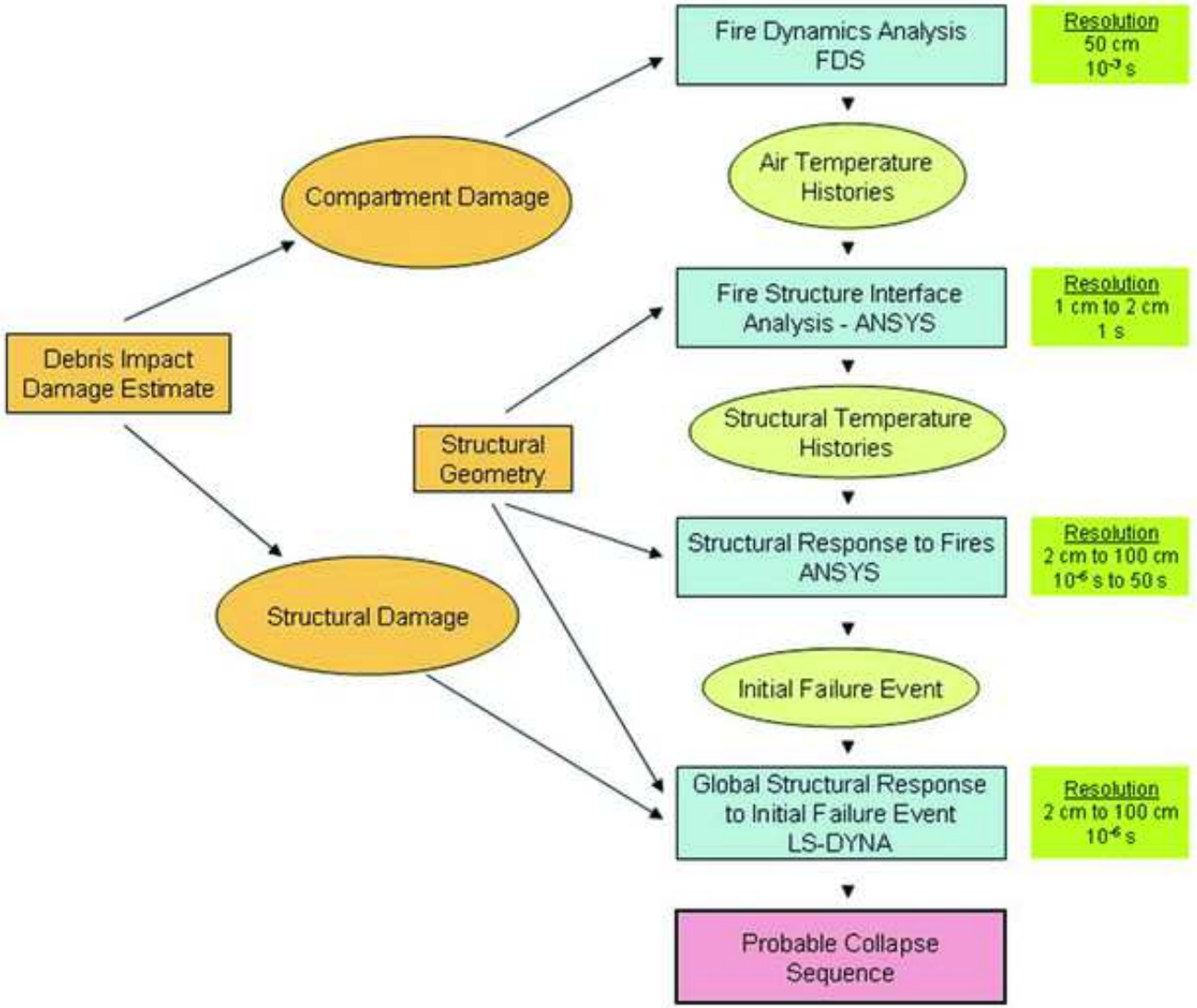

Journal of Structural Engineering. Submitted June 25, 2009; accepted February 16, 2011;
posted ahead of print February 18, 2011. doi:10.1061/(ASCE)ST.1943-541X.0000398

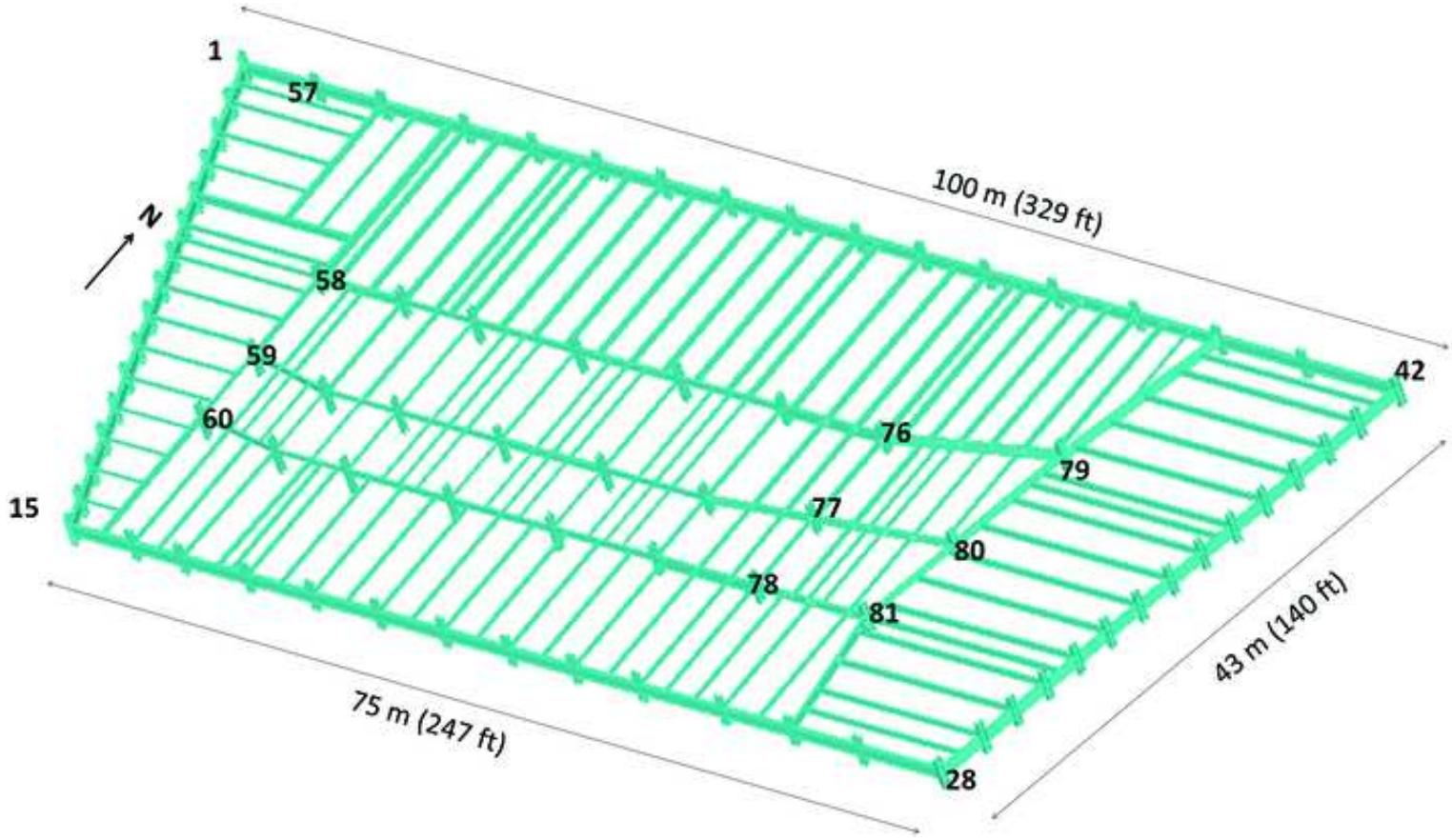

Journal of Structural Engineering. Submitted June 25, 2009; accepted February 16, 2011;
posted ahead of print February 18, 2011. doi:10.1061/(ASCE)ST.1943-541X.0000398

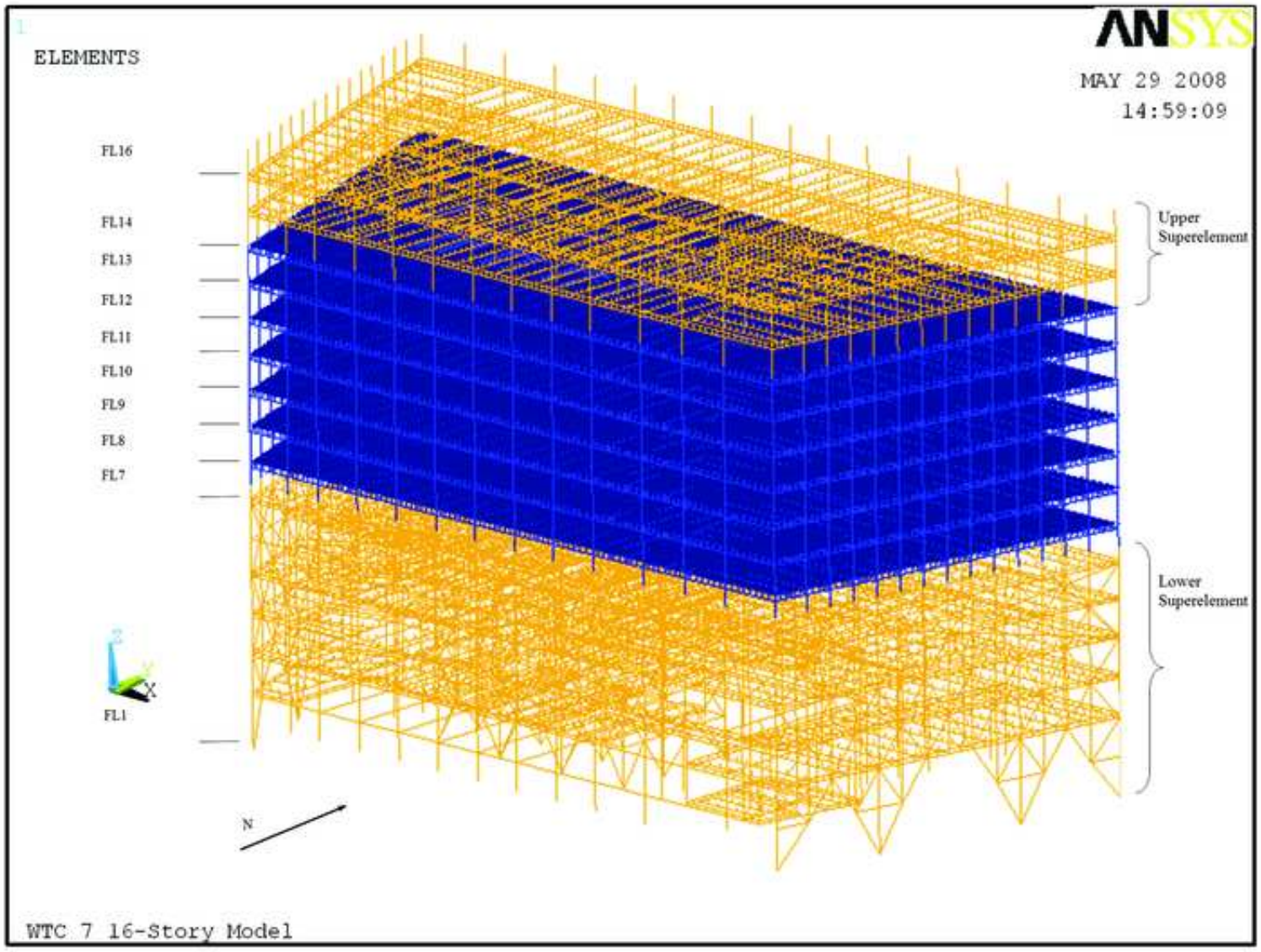

Journal of Structural Engineering. Submitted June 25, 2009; accepted February 16, 2011;
posted ahead of print February 18, 2011. doi:10.1061/(ASCE)ST.1943-541X.0000398

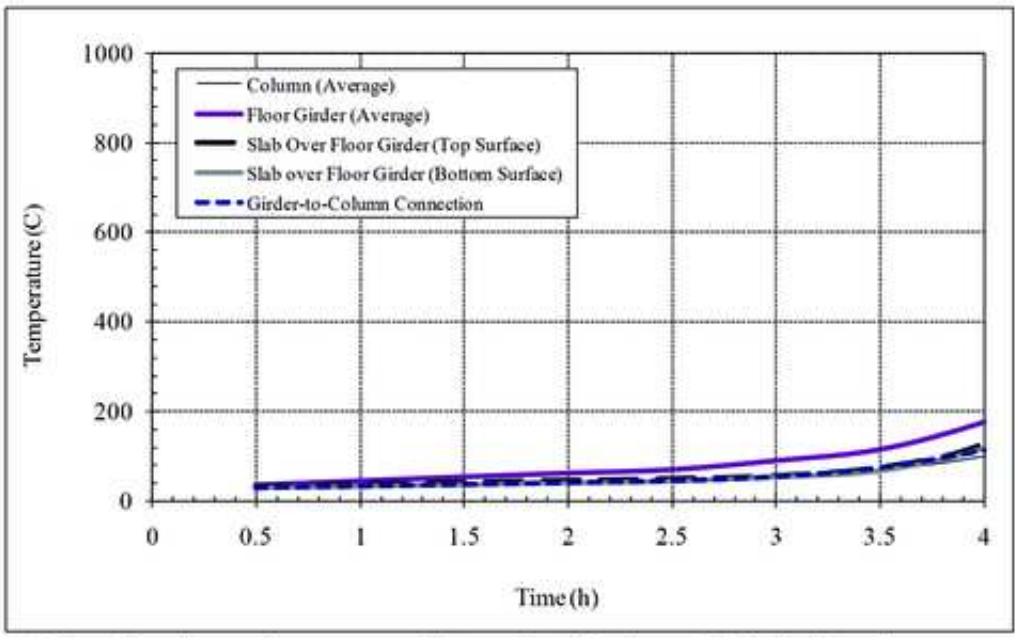

a) Floor framing and concrete slab north of Column 79 including floor girder, girder-to-column connection, slab and Column 79.

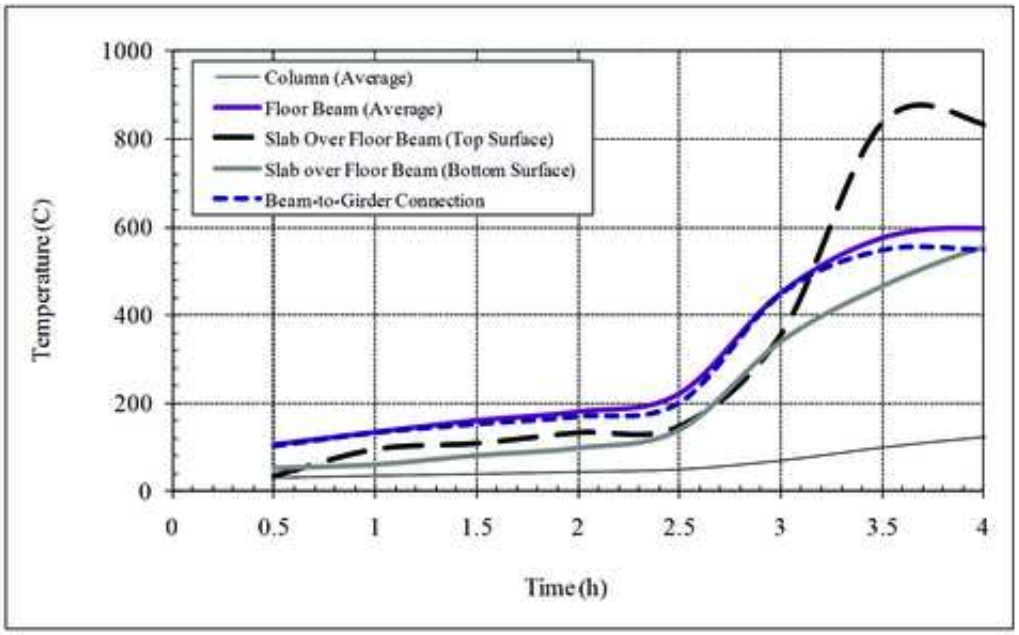

b) Floor framing and concrete slab south of Column 81 including floor beam, beam-to-girder connection, slab and Column 81.

Journal of Structural Engineering. Submitted June 25, 2009; accepted February 16, 2011;
posted ahead of print February 18, 2011. doi:10.1061/(ASCE)ST.1943-541X.0000398

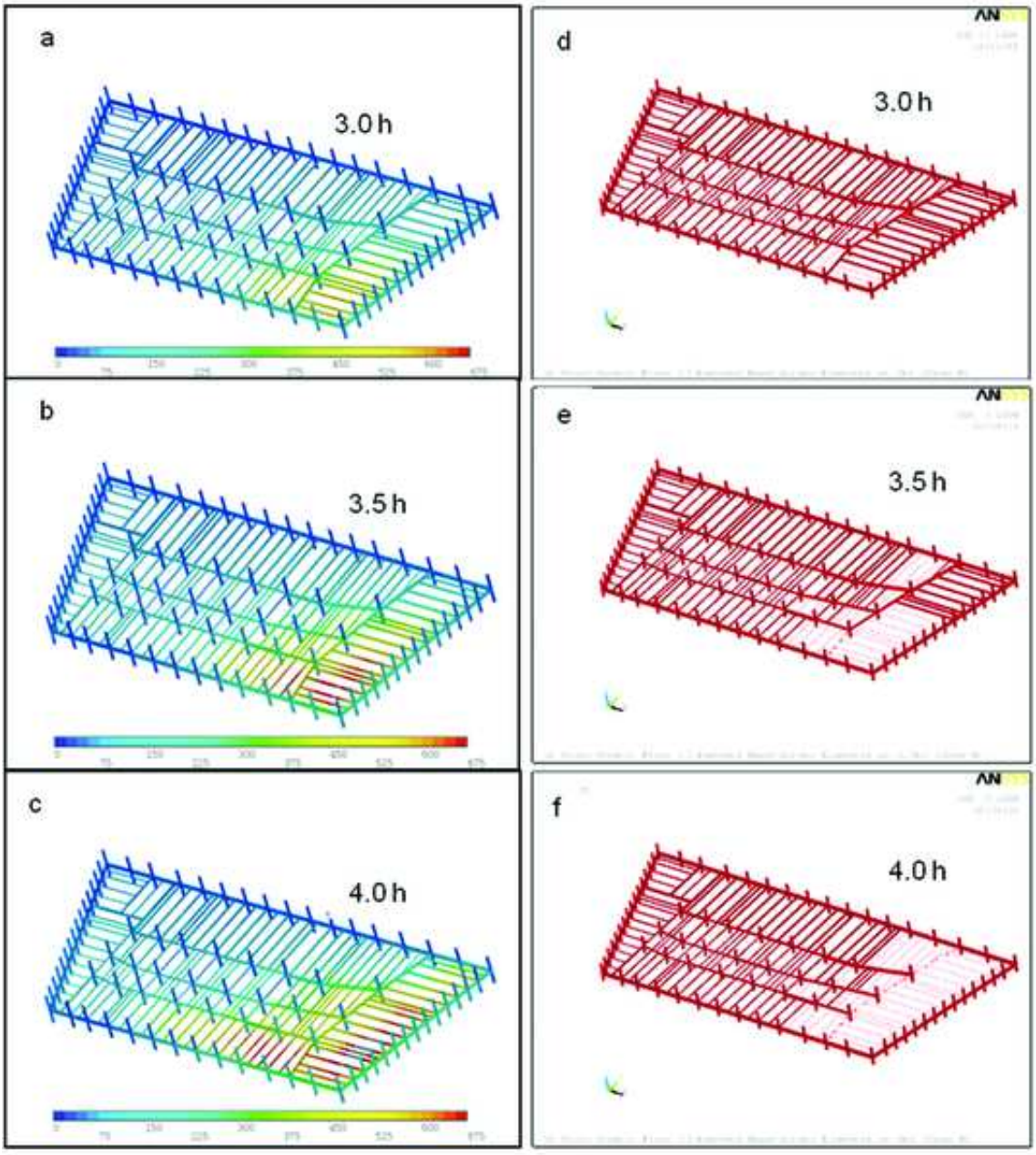

Journal of Structural Engineering. Submitted June 25, 2009; accepted February 16, 2011;
posted ahead of print February 18, 2011. doi:10.1061/(ASCE)ST.1943-541X.0000398

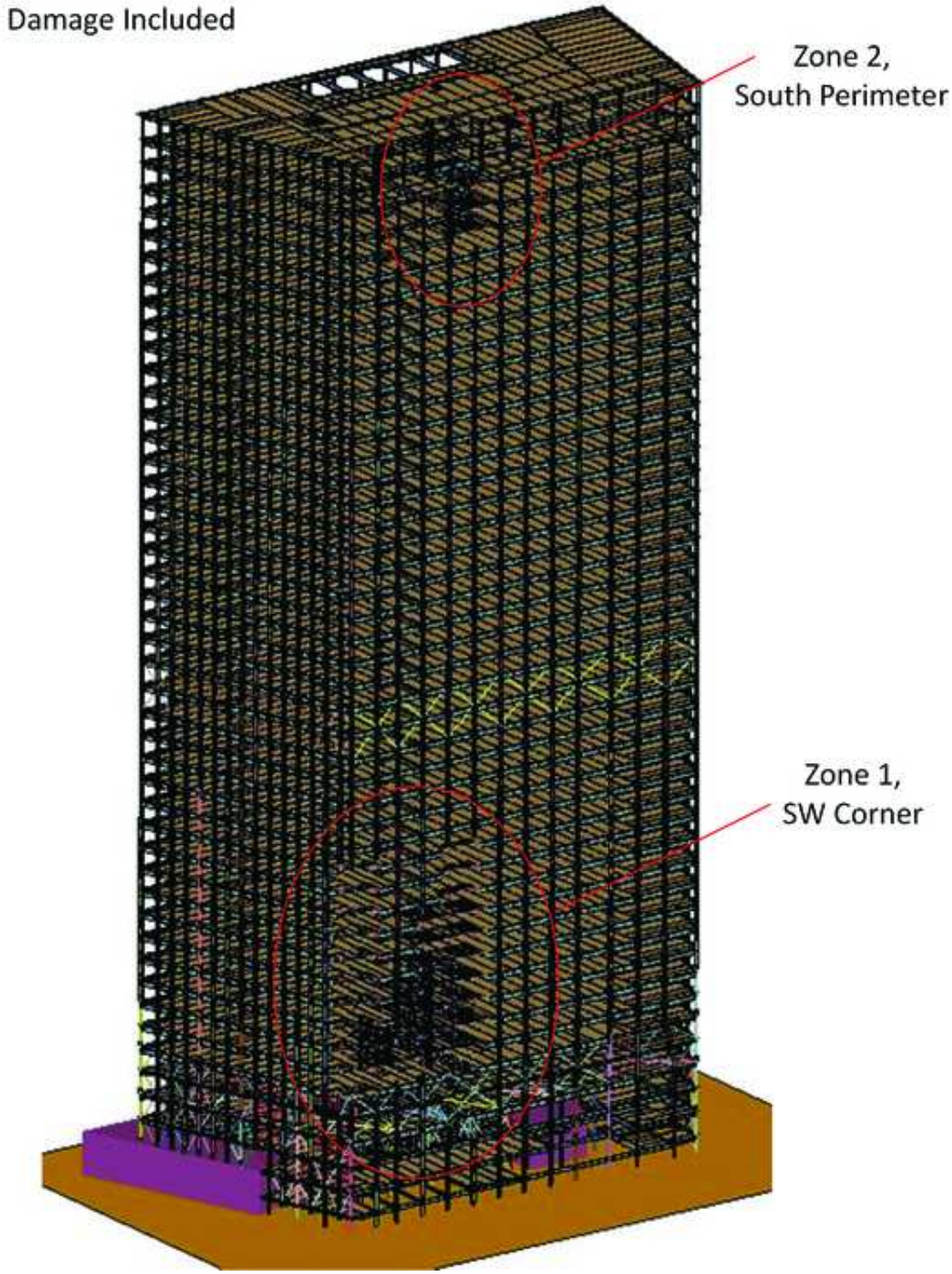

Journal of Structural Engineering. Submitted June 25, 2009; accepted February 16, 2011;
posted ahead of print February 18, 2011. doi:10.1061/(ASCE)ST.1943-541X.0000398

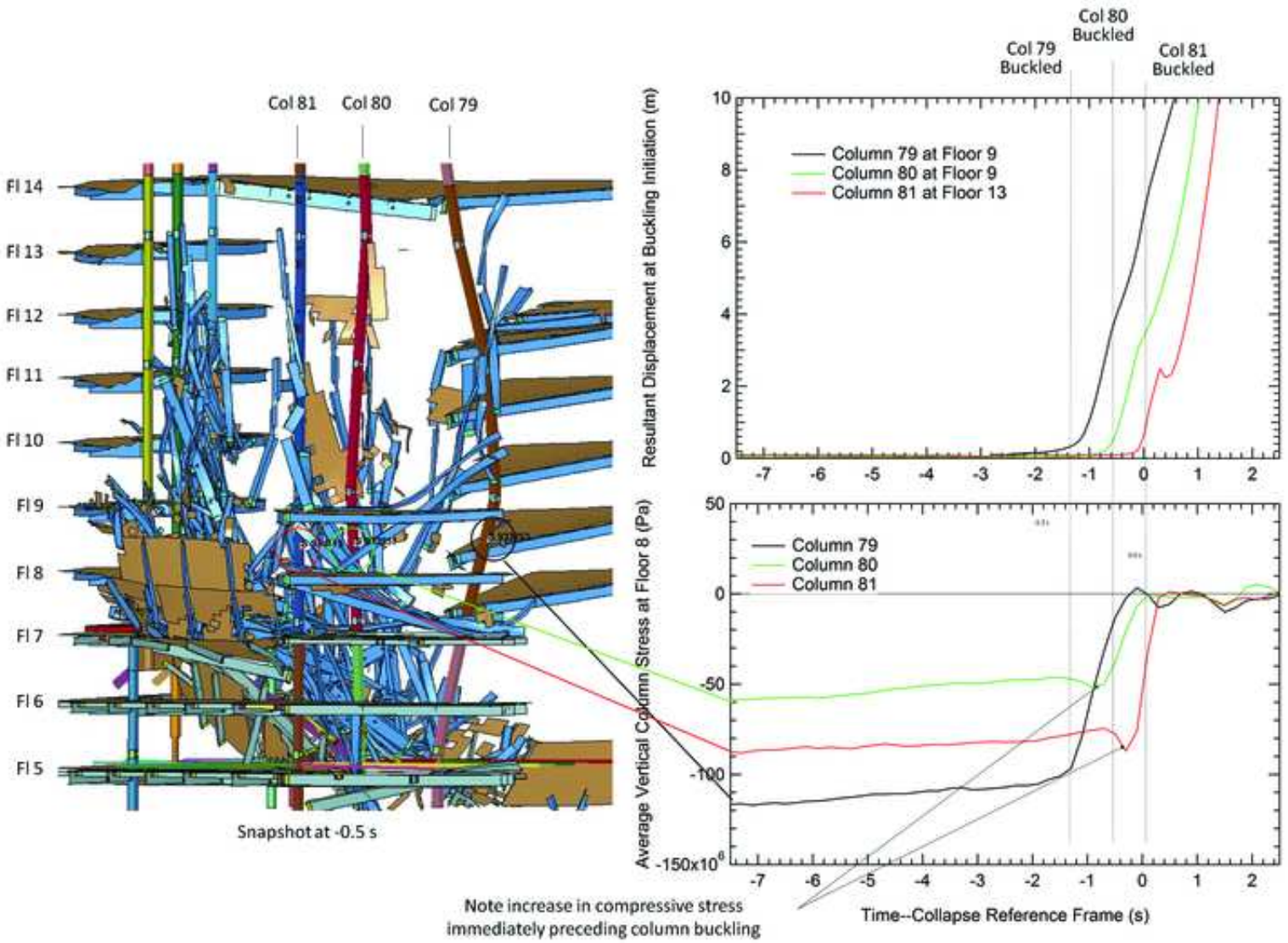

Journal of Structural Engineering. Submitted June 25, 2009; accepted February 16, 2011;
posted ahead of print February 18, 2011. doi:10.1061/(ASCE)ST.1943-541X.0000398

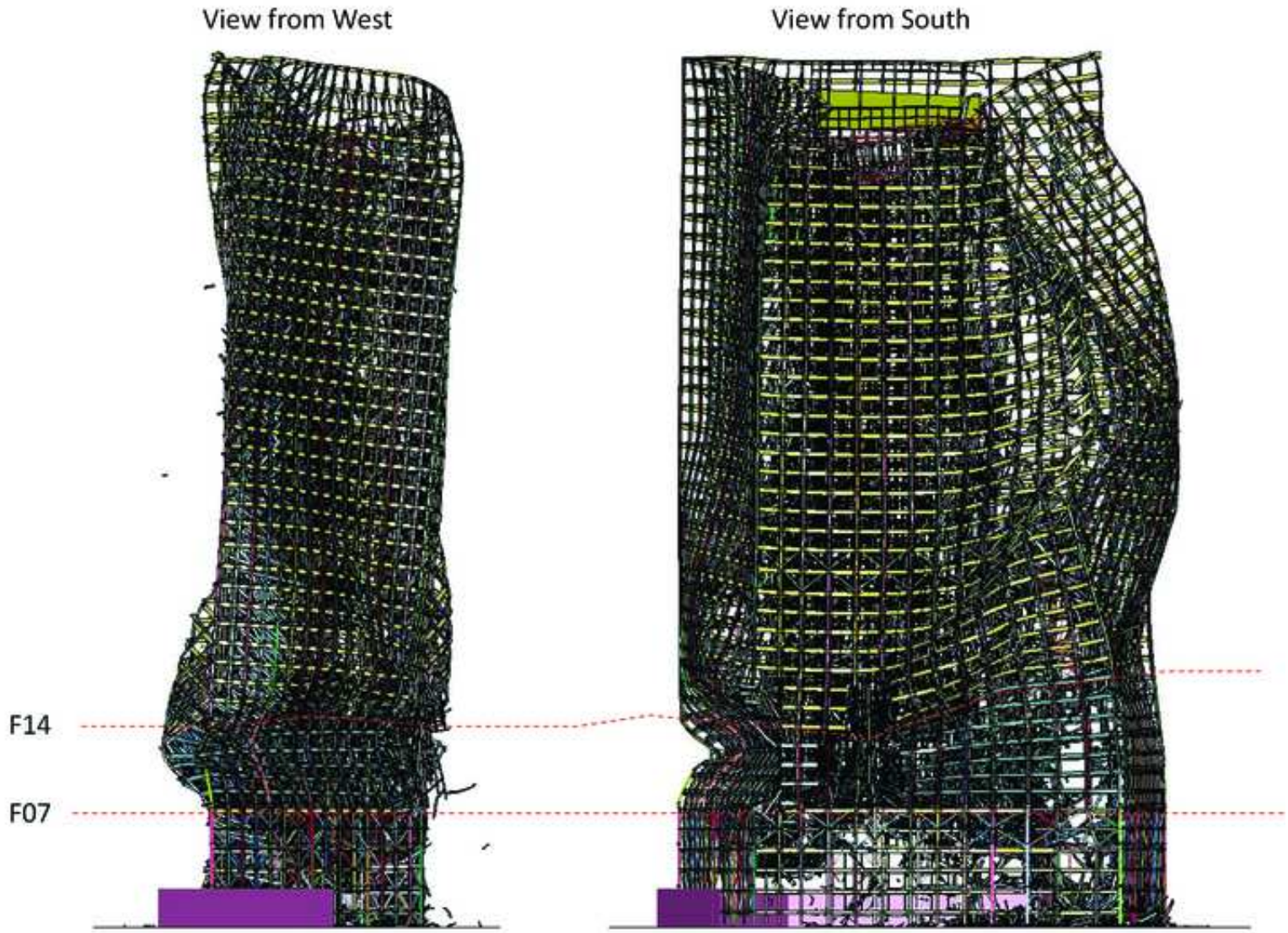

Journal of Structural Engineering. Submitted June 25, 2009; accepted February 16, 2011;
posted ahead of print February 18, 2011. doi:10.1061/(ASCE)ST.1943-541X.0000398

Table 1. Comparison of major collapse events: observed times versus analysis times for collapse analyses with and without debris impact damage.

Observation Time (s)	Analysis Time (s) with Debris Impact Damage	Analysis Time (s) without Debris Impact Damage	Event
≈ -6 s	-6.6 s	-6.6 s	Start of cascading floor failures around Column 79
Not available	-1.3	-1.4	Buckling of Column 79, quickly followed by buckling of Columns 80 and 81
0	≡ 0	≡ 0	Start of descent of east penthouse
2.0	2.4-2.7	2.3-2.6	Descent of east penthouse below roofline[a]
N/A	3.5-6.1	3.2-13.5	Buckling of columns across core, starting with Column 76
6.9	6.3	9.8	Initial downward motion of the north face roofline at the eastern section of building
8.5	7.3-7.7	8.7-9.2	Descent of the east end of the Screenwall below the roofline[a]
9.3	6.9,7.3	10.6,10.9	Descent of the west penthouse below the roofline[b]

a. 1st value was observed from the northwest and below, 2nd value was observed from the north at the roofline.

b. 1st value was observed in a video from the northwest below the roofline, 2nd value was observed in a video from the north at roofline.